ACES Asian Chemical Editorial Society

doi.org/10.1002/ajoc.202400625

ASIAN JOURNAL OF ORGANIC CHEMISTRY
Research Article

www.asianjoc.org

Synthesis of Tetraaryl Diazachrysenes by the Povarov Reaction and π Extension To Construct a Condensed Azaperylene Motif

Yuanrong Shan,[a] Takeshi Yasuda,[b] Takaki Kanbara,[a] and Junpei Kuwabara*[a, c]

Incorporating nitrogen into carbon-based materials can significantly modify their electronic properties. A comprehensive understanding of the structural and physical characteristics of aza-polycyclic aromatic hydrocarbons (aza-PAHs) is crucial for developing innovative materials. In this study, four aza-PAHs were synthesized using a combination of the Povarov reaction and intramolecular cyclization reaction by direct C–H arylation. The synthesized compounds were evaluated in terms of the crystal structure, photophysical properties, frontier energy levels, and hole-blocking properties in organic light-emitting diode (OLED). The intramolecular cyclization by direct C–H arylation afforded a condensed azaperylene molecule that exhibited long-wavelength absorption and emission, attributed to the high HOMO level resulting from π-extension.

Introduction

Aza-polycyclic aromatic hydrocarbons (aza-PAHs) are known for their unique optical and semiconducting properties.[1–6] The introduction of nitrogen atoms lowers the frontier orbital energy level of polycyclic aromatic hydrocarbons, enhancing their stability against oxidative degradation.[7–10] These features make aza-PAHs promising candidates for optoelectronic applications such as organic field-effect transistors (OFETs)[11–14] and organic light-emitting diodes (OLEDs).[15–22] Various synthetic strategies have been developed for aza-PAH production.[23–25] Recently, the Povarov reaction has been employed for the synthesis of aza-PAHs.[26–29] Initially used for synthesizing quinoline derivatives from aromatic amines, aldehydes, and alkenes (or alkynes).[30,31] Our group previously reported double and triple Povarov reactions involving aromatic diamines and triamines to obtain phenanthroline and triazatriphenylene derivatives, respectively.[26–28] Based on the previous results, we anticipated that the Povarov reaction of 1,5-naphthalenediamine would synthesize diazachrysene derivatives with extended π-conjugation (Figure 1 and Scheme 1). Chrysene, the parent skeleton of diazachrysene, is known for its high charge-carrier mobility and has been utilized in OFETs and OLEDs.[32–35] Incorporating nitrogen atoms into chrysene is anticipated to enhance its electron-transporting properties by lowering the energy levels. Azachrysene derivatives have been synthesized by several methods, including the Conrad–Impah reaction,[36] one-pot multicomponent reaction,[37] and photocatalytic synthesis.[38] On the other hand, intramolecular cyclization reactions, commonly used for π-conjugation extension, have been successful in producing new materials.[39–45] We hypothesized that the intramolecular cyclization of azachrysene would yield π-extended aza-PAHs. In general, intramolecular cyclization reactions are conducted using oxidative aromatic coupling,[46–48] alkali-metal-mediated reduction coupling,[49,50] or transition-metal-catalyzed coupling reactions.[41,51–53]

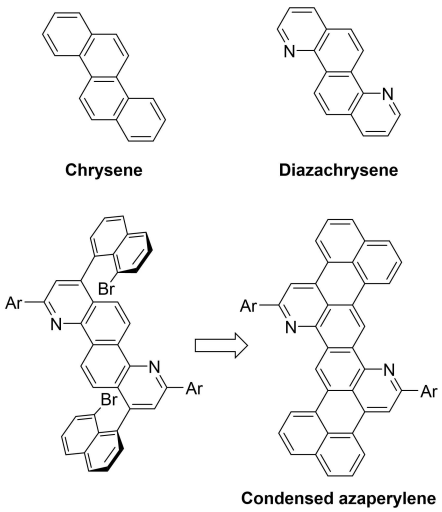

Figure 1. Top row: structures of chrysene and diazachrysene. Bottom row: synthetic strategy for a condensed azaperylene molecule.

[a] Y. Shan, T. Kanbara, J. Kuwabara
Institute of Pure and Applied Sciences, University of Tsukuba, 1–1–1 Tennodai, Tsukuba, Ibaraki 305–8573, Japan
E-mail: kuwabara@ims.tsukuba.ac.jp

[b] T. Yasuda
Research Center for Macromolecules and Biomaterials, National Institute for Materials Science (NIMS), 1–2–1 Sengen, Tsukuba, Ibaraki 305–0047, Japan

[c] J. Kuwabara
Tsukuba Research Center for Energy Materials Science (TREMS), Institute of Pure and Applied Sciences, University of Tsukuba, 1–1–1 Tennodai, Tsukuba, Ibaraki 305–8573, Japan

Supporting information for this article is available on the WWW under https://doi.org/10.1002/ajoc.202400625

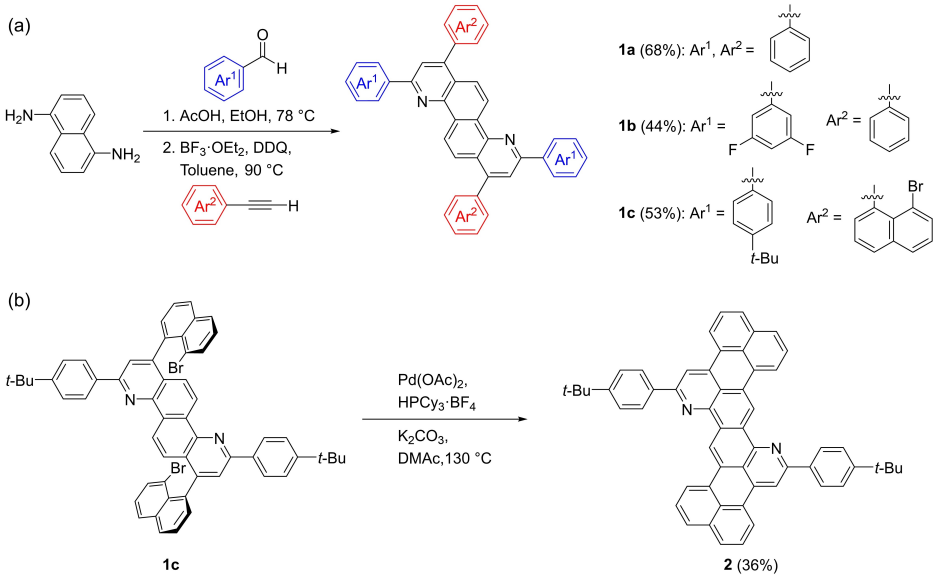

Scheme 1. (a) Synthesis of 4,10-diazachrysene derivatives by the Povarov reaction. (b) Synthesis of a condensed azaperylene molecule by direct arylation.

Each method offers distinct advantages for tailoring the optoelectronic properties of these materials. In intramolecular cyclization reactions of aza-PAHs, oxidative aromatic coupling is unsuitable due to their high oxidation potentials, while alkali-metal-mediated reduction reactions require harsh reaction conditions. Therefore, transition-metal-catalyzed coupling reactions represent the most viable approach. In this study, we employed an intramolecular direct C–H arylation reaction,[53–58] which requires only halogen groups for bond formation. Gorodetsky et al. reported the utility of this method in synthesizing nitrogen-containing rubicene and tetrabenzopentacene derivatives.[41] The primary objective of this study was to synthesize tetraphenyl-4,10-diazachrysene derivatives by the Povarov reaction and elucidate their physical properties. A secondary objective was to synthesize and characterize a condensed azaperylene molecule through the intramolecular cyclization of a diazachrysene derivative with Br substituents using a direct arylation reaction. In this study, we present the synthesis, physical properties, and electronic structure of aza-PAHs with extended π-conjugation.

Results and Discussion

Synthesis

To synthesize 1,3,7,9-tetraphenyl-4,10-diazachrysene (**1 a**), the double Povarov reaction was performed under previously reported conditions (Scheme 1).[26] The initial reaction between 1,5-naphthalenediamine and benzaldehyde, catalyzed by acetic acid, yielded a diimine intermediate (Figure S1, Supporting Information). Without isolating this intermediate, the reaction with phenylacetylene was subsequently conducted in the presence of $BF_3{\cdot}OEt_2$ and DDQ (2,3-dichloro-5,6-dicyano-1,4-benzoquinone). After purification by Soxhlet extraction, the target product **1 a** was obtained in a 68 % yield. The structure of **1 a** was confirmed using ^{1}H NMR spectroscopy, mass spectrometry, and elemental analysis (Figure S2). Similarly, a 3,5-difluorophenyl-substituted diazachrysene derivative (**1 b**) was synthesized to compare physical properties. The solubility of **1 b** was notably lower than that of **1 a** in common organic solvents such as chloroform and toluene. A bromonaphthalene-substituted diazachrysene derivative (**1 c**) was designed for intramolecular coupling, and *t*-Bu groups were introduced to the aryl groups to improve solubility. Compound **1 c** was prepared in a 53 % yield using the same method. Intramolecular direct arylation was investigated to optimize reaction conditions, yielding the target compound **2** in a 36 % yield (Scheme 1b). This is a straightforward method for the synthesis of aza-PAHs with extended π-conjugation. As the Povarov reaction[31] and the direct arylation reaction[54–59] are highly functional group tolerant, it is expected that a variety of related compounds can be synthesized using this method. Due to its high thermal stability, compound **2** was purified using Soxhlet extraction followed by sublimation at 350 °C.

Single-Crystal X-Ray Structure Analysis

The molecular structure of **1 a** was determined using single-crystal X-ray diffraction (Figure 2). The analysis revealed a highly planar diazachrysene core. The phenyl group (α) adjacent to the nitrogen exhibited a dihedral angle of 33.9° relative to the diazachrysene core, with the other phenyl group (β) having a larger dihedral angle of 51.7°, likely due to steric hindrance between the C–H groups of the β phenyl group and the diazachrysene core. The shortest distance between diazachrysene cores was 3.539 Å, indicating π-π stacking interactions in the crystal.[60,61] Compared to the π–π stacking observed in tetraphenyl-1,7-phenanthroline, synthesized similarly in a pre-

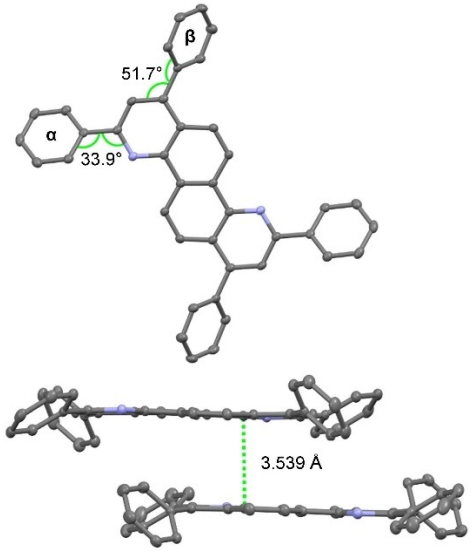

Figure 2. Molecular structure and packing diagrams of **1 a**.

vious study,[26,27] **1 a** demonstrated a greater degree of central unit overlap due to the large π conjugation of diazachrysene (Figure S7 and S8). The effective π–π stacking interactions in **1 a** are reminiscent of smooth carrier transport.

Physical Properties

UV-vis absorption and emission spectra were measured to investigate the physical properties of the diazachrysene derivatives (**1 a**, **1 b**) and condensed azaperylene molecules (**2**). Figure 3 shows the spectra for solutions and films prepared by vacuum deposition. The photophysical properties of **1 a** and **1 b** were found to be similar. The highest occupied molecular orbital (HOMO)-lowest unoccupied molecular orbital (LUMO) gap for both compounds is 3.03 eV, which is narrower than the gap observed in tetraphenyl-1,7-phenanthroline (3.55 eV) (Figure S7).[27] This narrowing is attributed to the extended π-conjugation of the diazachrysene core. Compound **2** displayed a redshift in both its maximum absorption wavelength (λ_{max}) and maximum emission wavelength (λ_{em}) compared to **1 a**, **1 b**, and **1 c** (Figures 3 and S14). The π-extension achieved via intramolecular cyclization reaction is responsible for this red shift.[43–45] A previously reported analog without nitrogen atoms (Figure S9) exhibited a λ_{em} of 534 nm, which is similar to that of compound **2** (544 nm).[50] This similarity suggests that the long-wavelength emission of compound **2** is likely due to the conjugated structure of its core. In addition, a significant red shift was observed especially in the thin film state, probably due to strong π–π stacking interaction resulting from the extended π-conjugation. The maximum emission wavelength of **2** reached 697 nm. Photoluminescence quantum yields (PLQYs) in the thin film state are summarized in Table 1. The reason compound **2** has the lowest PLQY is due to the energy gap law, where a smaller band gap results in a lower PLQY.[62] The PLQY of **1 b** is smaller than that of **1 a** because, as observed in the AFM image in Figure S12, the stronger aggregation tendency of **1 b** leads to aggregation-induced quenching.[63] Although **1 a** and **1 b** exhibited similar photophysical properties, their energy levels differed significantly. The electron-withdrawing effect of the F substituents in **1 b** resulted in lower HOMO and LUMO

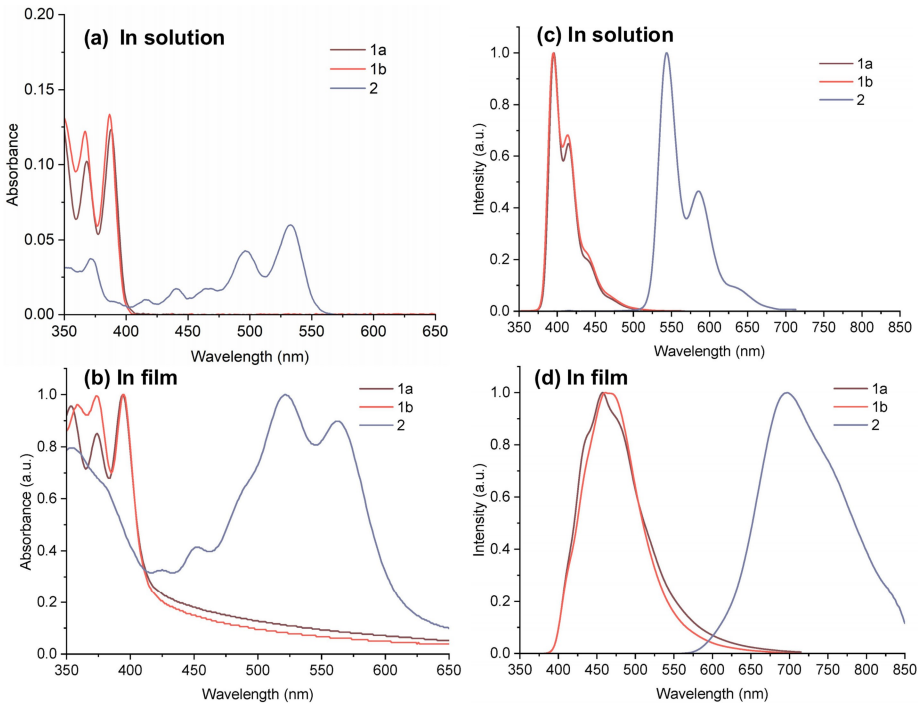

Figure 3. a: UV-vis absorption spectra of **1 a**, **1 b**, and **2** (in toluene, 5.0×10^{-6} M); **b**: UV-vis absorption spectra of **1 a**, **1 b**, and **2** (film state); **c**: Photoluminescence spectra (in toluene, 5.0×10^{-6} M); **d**: Photoluminescence spectra (film state).

Table 1. Physical properties of 4,10-diazachrysene derivatives.

	Solution state [a]			Thin-film state						
	λ_{abs}/nm		λ_{em}/nm	λ_{abs}/nm		λ_{em}/nm	PLQY/% [b]	$E_{g,opt}$/eV [c]	HOMO/eV [d]	LUMO/eV [e]
1a	388		395	394		457	19	3.03	−6.03	−3.00
1b	387		395	394		461	13	3.03	−6.42	−3.39
2	496	533	544	521	563	697	2	2.07	−5.04	−2.97

[a] in toluene, 5.0×10^{-6} M. [b] Photoluminescence Quantum Yield (PLQY). [c] Obtained from the absorption edge. [d] Obtained by photoelectron yield spectroscopy. [e] $E_{LUMO} = E_{g,opt} + E_{HOMO}$.

energy levels than **1a**. However, since both the HOMO and LUMO levels were affected similarly, the optical HOMO-LUMO gaps remained comparable in **1a** and **1b**. The HOMO and LUMO levels of a phenyl-substituted chrysene have been reported to be −5.79 and −2.53 eV, respectively (Figure S10).[64] Compound **1a** had lower HOMO and LUMO levels than the reference compound, revealing the effect of nitrogen incorporation. The HOMO level of compound **2** was higher than that of compound **1a**, though their LUMO levels were comparable. This elevated HOMO level is responsible for the narrow optical band gap in compound **2**. The high HOMO level of compound **2** is further discussed in the density functional theory (DFT) calculations section.

DFT Calculation

To investigate the electronic structures of compounds **1a**, **1b**, and **2**, DFT calculations were performed at the B3LYP/6–31G(d) level of theory. The calculated HOMO of **1a** and **2** are shown in Figure 4. For compound **2**, the HOMO was also distributed at sites extended by the intramolecular cyclization. In contrast, the HOMO of **1a** was not distributed to the phenyl groups, likely due to the significant twisting of the phenyl group, which was also observed in its crystal structure (Figure 2, β phenyl group). The aromaticity of **2** was evaluated using nucleus-independent chemical shift (NICS) calculations (Figure 5).[65,66] The results showed that ring b exhibited low aromaticity, consistent with observations for perylene. In addition, the ^{1}H NMR chemical shifts of compound **2** and perylene showed high similarity (Figure S15). Based on these results, compound **2** can be viewed as a nitrogen-containing perylene derivative with a condensed structure sharing one edge.

Evaluation as a Hole-Blocking Material in OLED

Compounds **1a** and **1b** were evaluated as hole-blocking materials in OLED devices due to their relatively low HOMO levels and the possibility of large-scale synthesis (Figure 6). OLEDs with identical device configurations to those in previous studies were fabricated to enable direct performance comparisons with previously synthesized compounds (see Experimental section for details). The OLED device containing **1a** exhibited an external quantum efficiency (EQE) of 1.43%, whereas the

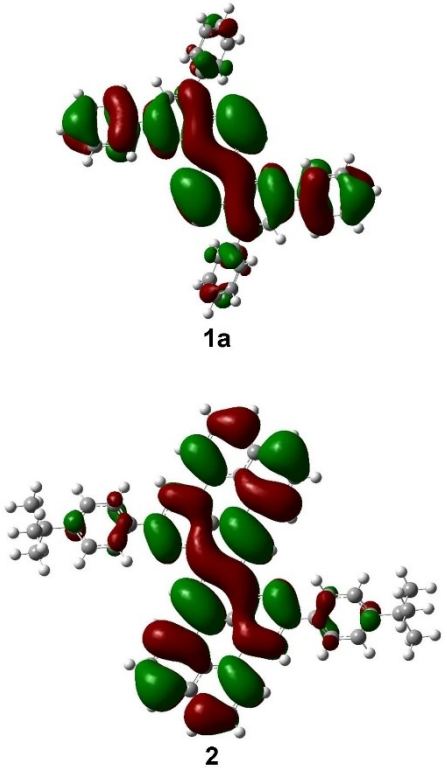

Figure 4. Highest occupied molecular orbital (HOMO) of compounds **1a** and **2**, obtained by density functional theory (DFT) calculation at the B3LYP/6–31G(d) level of theory.

device containing **1b** did not function as expected. The failure of the device with **1b** was attributed to the inability of the compound to form a uniform film due to its high cohesion (Figure S12). The high cohesion of **1b** was also confirmed in the lower solubility in toluene ($c = 1.1\times10^{-5}$ M) than **1a** ($c = 4.2\times10^{-4}$ M). The EQE of the device without **1a** showed an EQE of only 0.32%,[26,27] confirming that **1a** functioned as a hole-blocking material. The EQE value of the device with **1a** (1.43%) was lower than that of the device containing 1,7-phenanthroline derivative (2.4%).[26,27] The higher HOMO level of **1a** (−6.03 eV) compared to the 1,7-phenanthroline derivative (−6.38 eV) likely accounts for its low performance of **1a** as a hole-blocking material. While it was expected that the extended π-conjugation of diazachrysene would improve device performances through improved carrier mobility, the HOMO level

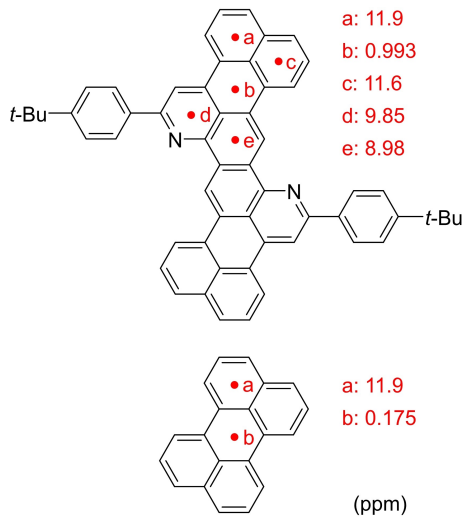

Figure 5. Nucleus-independent chemical shift (NICS(1)) values (ppm) of compound **2** and perylene obtained by DFT calculation at the B3LYP/6–31G(d) level of theory.

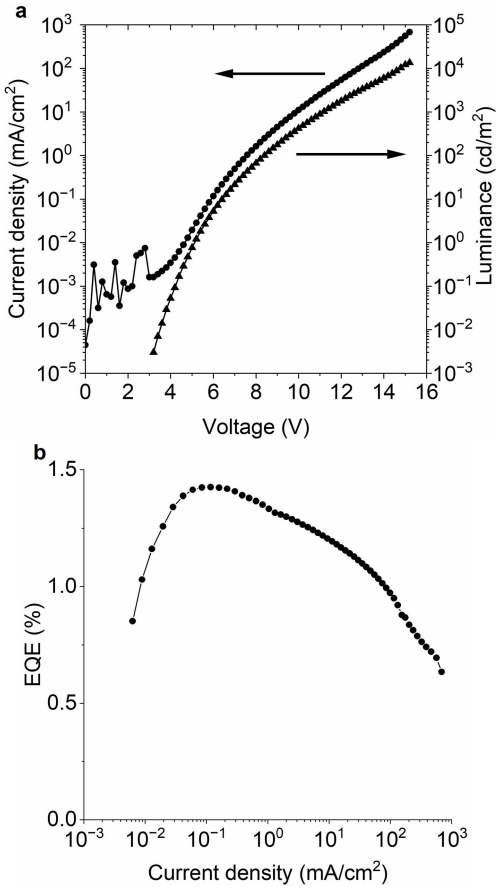

Figure 6. (a) Current density–luminance–voltage characteristics. (b) External quantum efficiency (EQE) versus current density of the OLED device with compound **1 a**. Configuration: Glass/ITO/PEDOT:PSS (40 nm)/Green light-emitting spiro-copolymer (33 nm)/**1 a** (40 nm)/LiF (1 nm)/Al (100 nm).

significantly influenced the overall efficiency of the device performance.

Conclusions

In this study, four aza-PAHs were synthesized by the Povarov reaction and intramolecular cyclization reaction employing direct C–H arylation. Single crystal X-ray structure analysis of 1,3,7,9-tetraphenyl-4,10-diazachrysene (**1 a**) revealed the high planarity of the diazacrylene backbone and the presence of π–π stacking. Compound **1 a** exhibited good film-forming properties and acted as a hole-blocking material in OLEDs. The intramolecular cyclization of the diazachrysene derivative with Br substituents by direct arylation reaction resulted in the formation of π-extended aza-PAHs bearing 10 fused benzene rings. Due to its large π-conjugation, this compound displayed long-wavelength absorption and emission, with a maximum emission wavelength of 697 nm in the film state. DFT calculations were used to estimate the electronic structure, demonstrating that the compound could be regarded as a fused ring of perylene containing nitrogen. The condensed azaperylene motif represents a novel structural configuration among aza-PAHs. This study provides a fundamental understanding of the synthesis of π-extended aza-PAHs and their structure-property relationships, contributing to for the design for organic optoelectronic materials.

Experimental Section

Synthesis of 1 a

A mixture of 1,5-diaminonaphthalene (475 mg, 3.00 mmol), benzaldehyde (637 mg, 6.00 mmol) and acetic acid (1 drop) in dried ethanol (15 mL) was stirred at 78 °C for 2 h under nitrogen atmosphere. After the reaction, volatiles were removed under vacuum. The phenylacetylene (988 μL, 9.00 mmol), 2,3-dichloro-5,6-dicyano-1,4-benzoquinone (DDQ, 1498 mg, 6.60 mmol), $BF_3{\cdot}OEt_2$ (889 μL, 7.20 mmol), and dried toluene (30 mL) were added to the mixture. The reaction mixture was stirred at 90 °C for 72 h under nitrogen atmosphere. After the reaction, toluene and $BF_3{\cdot}OEt_2$ were removed under vacuum at 60 °C. The crude product was transferred to a Soxhlet extractor and washed with methanol for 9.5 h and then acetone for 2 h at the reflux temperature. The product was extracted with $CHCl_3$ at the reflux temperature. After the removal of $CHCl_3$, light yellow solid (**1 a**) was obtained (1065 mg, yield 68 %). The analytically pure sample was obtained by sublimation purification. ^{1}H NMR (400 MHz, $CDCl_3$) $\delta = 9.61$ (d, 1H, $J = 8.8$ Hz), 8.40 (d, 2H, $J = 7.2$ Hz), 8.16 (d, 1H, $J = 9.2$ Hz), 8.04 (s, 1H), 7.67 (d, 2H, $J = 6.4$ Hz), 7.56 (m, 6H). Anal. Calcd. for $C_{40}H_{26}N_2$: C, 89.86; H, 4.90; N, 5.24; Found: C, 89.69; H, 4.85; N, 5.21. MALDI-TOF-MS Calcd. for $C_{40}H_{26}N_2$ (M^+) 534, Found 534.

1 b: Light yellow solid (804 mg, yield 44 %). ^{1}H NMR (600 MHz, $CDCl_2CDCl_2$, 373 K) $\delta = 9.54$ (d, 1H, $J = 9.0$ Hz), 8.13 (d, 1H, $J = 9.6$ Hz), 7.91 (m, 3H), 7.57 (m, 5H), 6.90 (m, 1H). Anal. Calcd. for $C_{40}H_{22}F_4N_2$: C, 79.20; H, 3.66; F, 12.53; N, 4.62; Found: C, 79.44; H, 3.62; N, 4.79.

1 c: Light yellow solid (1024 mg, yield 53 %). ^{1}H NMR (600 MHz, $CDCl_3$) $\delta = 9.52$ (d, 1H, $J = 9.0$ Hz), 8.30 (d, 2H, $J = 9.0$ Hz), 8.03 (dd, 1H, $J = 1.2$, 8.4 Hz), 8.05 (s, 1H), 8.04 (dd, 1H, $J = 0.8$, 5.2 Hz), 7.76 (dd, 1H, $J = 1.3$, 7.3 Hz), 7.67 (t, 1H, $J = 7.6$ Hz), 7.53 (dd, 1H, $J = 1.4$, 7.0 Hz), 7.57 (d, 1H, $J = 9.0$ Hz), 7.54 (d, 2H, $J = 8.6$ Hz), 7.38 (t, 1H, $J = 7.8$ Hz), 1.38 (s, 9H). Anal. Calcd. for $C_{56}H_{44}Br_2N_2$: C, 74.34; H, 4.90;

Br, 17.66; N, 3.10; Found: C, 74.45; H, 4.84; N, 3.01. MALDI-TOF-MS Calcd. for $C_{56}H_{44}Br_2N_2$: (M^+) 904, Found 904.

Synthesis of 2

A mixture of **1 c** (54 mg, 0.06 mmol), $Pd(OAc)_2$ (2.7 mg, 0.012 mmol), tricyclohexylphosphonium tetrafluoroborate (8.8 mg, 0.024 mmol), and potassium carbonate (66 mg, 0.48 mmol) in dried dimethylacetamide (6.8 mL) was stirred at 130 °C for 72 h under nitrogen atmosphere. After the reaction, dimethylacetamide was removed under vacuum at 60 °C. The crude product was transferred to a Soxhlet extractor and washed with methanol and *n*-hexane at the reflux temperature until the extracted solution exhibited no coloration. The crude product was extracted with $CHCl_3$ at the reflux temperature. The diluted solution of the products in $CHCl_3$ was purified by passing through silica gel. The product was isolated by recrystallization by heating solution in *o*-dichlorobenzene to 150 °C and returning to room temperature. The analytically pure sample was obtained by sublimation purification at 350 °C. **2**: dark red solid (16.2 mg, yield 36 %). ^{1}H NMR (600 MHz, $CDCl_2CDCl_2$, 373 K) $\delta = 10.11$ (s, 1H), 8.63 (d, 1H, $J = 6.0$ Hz), 8.54 (s, 1H), 8.37 (d, 3H, overlap, $J = 7.8$ Hz), 7.85 (d, 1H, $J = 7.2$ Hz), 7.78 (d, 1H, $J = 9.0$ Hz), 7.67 (d, 2H, $J = 7.8$ Hz), 7.63 (t, 1H, $J = 6.3$ Hz), 7.56 (t, 1H, $J = 6.9$ Hz), 1.47 (s, 9H). Anal. Calcd. for $C_{56}H_{42}N_2$: C, 90.53; H, 5.70; N, 3.77; Found: C, 90.49; H, 5.47; N, 3.71. MALDI-TOF-MS Calcd. for $C_{56}H_{42}N_2$: (M^+) 742, Found 742.

Fabrication and Characterization of OLEDs

OLEDs were fabricated in the following configuration: ITO/PEDOT:PSS/emitting layer (Green light-emitting spiro-copolymer)/electron-transporting and hole-blocking layer (**1 a**)/LiF/Al. The patterned indium tin oxide (ITO) glass (conductivity: 10 Ω/square) was pre-cleaned in an ultrasonic bath of acetone and ethanol and then treated in an ultraviolet-ozone chamber. A thin layer (40 nm) of PEDOT:PSS was spin-coated onto the ITO at 3000 rpm and air-dried at 110 °C for 10 min on a hot plate. The substrate was then transferred to a N_2-filled glove box where it was re-dried at 110 °C for 10 min on a hot plate. A toluene solution of Green light-emitting spiro-copolymer (4 mg/1 mL) was subsequently spin-coated onto the PEDOT:PSS surface to form the light-emitting layer with the thicknesses of 33 nm and the light-emitting layer was dried at 80 °C for 10 min. **1 a** (40 nm), LiF (1 nm) and Al (100 nm) were then deposited onto the active layer with conventional thermal evaporation at a chamber pressure lower than 5×10^{-4} Pa, which provided the devices with an active area of 2×2 mm^2. Current-voltage characteristics and luminance of the OLED were simultaneously measured using an ADCMT 6245 DC voltage current source/monitor (ADC CORPORATION) and an LS-100 luminance meter (KONICA MINOLTA, INC.), respectively. The EL spectra were measured using an array spectrometer (MCPD-9800–311 C, Otsuka Electronics Co, Ltd.).

Supporting Information Summary

Electronic Supplementary Information (ESI) available: Supplementary figures, computational details, and crystallographic data in CIF. CCDC 2393382.

Acknowledgements

The authors thank the Chemical Analysis Center of the University of Tsukuba for the measurements of NMR, the single-crystal X-ray diffraction, and MALDI-TOF-MS. The authors are grateful to Riken Keiki Co. Ltd. for measurements of photo-electron yield spectroscopy using an AC-3 spectrometer. The authors thank Dr. A. Takai for their assistance with the mass spectrometry. This work was partially supported by JSPS KAKENHI Grant Number JP22K05075, JP23K04884, Iketani Science and Technology Foundation, and JST SPRING, Japan Grant Number JPMJSP2124.

Conflict of Interests

The authors declare no conflict of interest.

Data Availability Statement

The data that support the findings of this study are available from the corresponding author upon reasonable request.

Keywords: Povarov reaction · Diazachrysenes · Condensed azaperylene · Hole-blocking material

[1] Y. Takeda, P. Data, S. Minakata, *Chem. Commun.* **2020**, *56*, 8884–8894.
[2] W. Zong, N. Hippchen, B. Dittmar, M. Elter, P. Ludwig, F. Rominger, J. Freudenberg, U. H. Bunz, *Asian J. Org. Chem.* **2023**, *12*, e202300462.
[3] H. Xin, J. Li, R.-Q. Lu, X. Gao, T. M. Swager, *J. Am. Chem. Soc.* **2020**, *142*, 13598–13605.
[4] M. Krzeszewski, D. Gryko, D. T. Gryko, *Acc. Chem. Res.* **2017**, *50*, 2334–2345.
[5] U. H. F. Bunz, *Acc. Chem. Res.* **2015**, *48*, 1676–1686.
[6] U. H. Bunz, J. Freudenberg, *Acc. Chem. Res.* **2019**, *52*, 1575–1587.
[7] H. Ye, D. Chen, M. Liu, S. J. Su, Y. F. Wang, C. C. Lo, A. Lien, J. Kido, *Adv. Funct. Mater.* **2014**, *24*, 3268–3275.
[8] X.-Y. Wang, X. Yao, A. Narita, K. Müllen, *Acc. Chem. Res.* **2019**, *52*, 2491–2505.
[9] C. J. Tonzola, M. M. Alam, W. Kaminsky, S. A. Jenekhe, *J. Am. Chem. Soc.* **2003**, *125*, 13548–13558.
[10] T. Kirschbaum, F. Rominger, M. Mastalerz, *Chem. Eur. J.* **2020**, *26*, 14560–14564.
[11] K. Tajima, K. Matsuo, H. Yamada, S. Seki, N. Fukui, H. Shinokubo, *Angew. Chem.* **2021**, *133*, 14179–14186.
[12] S. Miao, A. L. Appleton, N. Berger, S. Barlow, S. R. Marder, K. I. Hardcastle, U. H. Bunz, *Chem. Eur. J.* **2009**, *15*, 4990–4993.
[13] Z. Liang, Q. Tang, J. Xu, Q. Miao, *Adv. Mater.* **2011**, *23*, 1535–1539.
[14] E. Ahmed, A. L. Briseno, Y. Xia, S. A. Jenekhe, *J. Am. Chem. Soc.* **2008**, *130*, 1118–1119.
[15] T. Yasuda, K. Sakamoto, *Jpn. J. Appl. Phys.* **2024**, *63*, 10SP12.
[16] T. Tsutsui, N. Takada, *Jpn. J. Appl. Phys.* **2013**, *52*, 110001.
[17] H. Nakanotani, Y. Tsuchiya, C. Adachi, *Chem. Lett.* **2021**, *50*, 938–948.
[18] A. P. Kulkarni, C. J. Tonzola, A. Babel, S. A. Jenekhe, *Chem. Mater.* **2004**, *16*, 4556–4573.
[19] R. Komatsu, H. Sasabe, J. Kido, *J. Photonics Energy* **2018**, *8*, 032108.
[20] H. Fukagawa, K. Suzuki, H. Ito, K. Inagaki, T. Sasaki, T. Oono, M. Hasegawa, K. Morii, T. Shimizu, *Nat. Commun.* **2020**, *11*, 3700.
[21] S. M. Elbert, E. Bolgert, O. T. Paine, F. Ghalami, W.-S. Zhang, U. Zschieschang, F. Rominger, D. Popp, H. Klauk, M. Elstner, *Org. Chem. Front.* **2024**, *11*, 5340–5349.
[22] T. Earmme, E. Ahmed, S. A. Jenekhe, *Adv. Mater.* **2010**, *22*, 4744–4748.
[23] M. Li, Y. Yuan, Y. Chen, *Chin. J. Chem.* **2021**, *39*, 3101–3115.
[24] Q. Tan, H. Chen, H. Xia, B. Liu, B. Xu, *Chem. Commun.* **2016**, *52*, 537–540.

[25] N. Ukwitegetse, P. J. G. Saris, J. R. Sommer, R. M. Haiges, P. I. Djurovich, M. E. Thompson, *Chem. Eur. J.* **2019**, *25*, 1472–1475.
[26] S. Yamamoto, Z. Y. Zhou, G. Hiruta, K. Takeuchi, J.-C. Choi, T. Yasuda, T. Kanbara, J. Kuwabara, *J. Org. Chem.* **2021**, *86*, 7920–7927.
[27] S. Yamamoto, T. Yasuda, T. Kanbara, J. Kuwabara, *Bull. Chem. Soc. Jpn.* **2022**, *95*, 458–465.
[28] S. Yamamoto, N. Ishida, T. Yasuda, T. Kanbara, J. Kuwabara, *Asian J. Org. Chem* **2023**, *12*, e202300181.
[29] E. R. Peng, A. M. Burke, D. J. Dibble, R. Kurakake, P. Liu, R. Lopez, P. R. Dennison, A. A. Gorodetsky, *RSC Adv.* **2024**, *14*, 28475–28486.
[30] R. G. Savchenko, R. M. Limantceva, S. L. Khursan, K. S. Mesheriakova, A. G. Tolstikov, V. N. Odinokov, *J. Heterocycl. Chem.* **2022**, *59*, 2025–2036.
[31] V. V. Kouznetsov, *Tetrahedron* **2009**, *65*, 2721–2750.
[32] J. Chatsirisupachai, T. Sudyoadsuk, S. Namuangrak, V. Promarak, *Synlett* **2022**, *33*, 1419–1425.
[33] S. Kang, H. Lee, H. Jung, M. Jo, M. Jung, J. Park, *Dyes Pigm.* **2018**, *156*, 299–306.
[34] H. Shin, H. Jung, B. Kim, J. Lee, J. Moon, J. Kim, J. Park, *J. Mater. Chem. C* **2016**, *4*, 3833–3842.
[35] T.-L. Wu, H.-H. Chou, P.-Y. Huang, C.-H. Cheng, R.-S. Liu, *J. Org. Chem.* **2014**, *79*, 267–274.
[36] I. Opsenica, J. C. Burnett, R. Gussio, D. Opsenica, N. Todorovic, C. A. Lanteri, R. J. Sciotti, M. Gettayacamin, N. Basilico, D. Taramelli, *J. Med. Chem.* **2011**, *54*, 1157–1169.
[37] T. Ataee-Kachouei, M. Nasr-Esfahani, I. M. Baltork, V. Mirkhani, M. Moghadam, S. Tangestaninejad, R. Kia, *ChemistrySelect* **2019**, *4*, 2301–2306.
[38] L.-L. Su, Y.-W. Zheng, W.-G. Wang, B. Chen, X.-Z. Wei, L.-Z. Wu, C.-H. Tung, *Org. Lett.* **2022**, *24*, 1180–1185.
[39] Y. Zhang, S. H. Pun, Q. Miao, *Chem. Rev.* **2022**, *122*, 14554–14593.
[40] X. Tian, K. Shoyama, F. Würthner, *Chem. Sci.* **2023**, *14*, 284–290.
[41] Y. S. Park, D. J. Dibble, J. Kim, R. C. Lopez, E. Vargas, A. A. Gorodetsky, *Angew. Chem. Int. Ed.* **2016**, *55*, 3352–3355.
[42] M. Grzybowski, B. Sadowski, H. Butenschön, D. T. Gryko, *Angew. Chem. Int. Ed.* **2020**, *59*, 2998–3027.
[43] K. Shoyama, F. Würthner, *Org. Chem. Front.* **2025**, *12*, 328–345.
[44] H. Ito, K. Ozaki, K. Itami, *Angew. Chem. Int. Ed.* **2017**, *56*, 11144–11164.
[45] B. Szymański, S. R. Sahoo, R. Valiev, O. Vakuliuk, P. Łaski, K. N. Jarzembska, R. Kamiński, G. Baryshnikov, M. B. Teimouri, D. T. Gryko, *New J. Chem.* **2024**, *48*, 2416–2420.
[46] M. Krzeszewski, D. T. Gryko, *J. Org. Chem.* **2015**, *80*, 2893–2899.
[47] M. Krzeszewski, P. Świder, Ł. Dobrzycki, M. K. Cyrański, W. Danikiewicz, D. T. Gryko, *Chem. Commun.* **2016**, *52*, 11539–11542.
[48] S. Mishra, M. Krzeszewski, C. A. Pignedoli, P. Ruffieux, R. Fasel, D. T. Gryko, *Nat. Commun.* **2018**, *9*, 1714.
[49] D. T. Gryko, J. Piechowska, M. Gałęzowski, *J. Org. Chem.* **2010**, *75*, 1297–1300.
[50] K. Fujishiro, Y. Morinaka, Y. Ono, T. Tanaka, L. T. Scott, H. Ito, K. Itami, *J. Am. Chem. Soc.* **2023**, *145*, 8163–8175.
[51] K. Parthasarathy, M. Jeganmohan, C.-H. Cheng, *Org. Lett.* **2008**, *10*, 325–328.
[52] D. Shabashov, O. Daugulis, *J. Org. Chem.* **2007**, *72*, 7720–7725.
[53] Z. Zhang, D. Csòkás, I. Fernández, M. C. Stuparu, *Chem* **2024**, *10*, 3199–3211.
[54] L.-C. Campeau, K. Fagnou, *Chem. Commun.* **2006**, 1253–1264.
[55] M. Kato, N. Fukui, H. Shinokubo, *Chem. Lett.* **2022**, *51*, 288–291.
[56] B. Bouzayani, R. Ben Salem, J. F. Soulé, H. Doucet, *Eur. J. Org. Chem.* **2019**, *2019*, 4581–4588.
[57] K. Takagi, Y. Hirano, K. Mikami, S. Kikkawa, I. Azumaya, *Eur. J. Org. Chem.* **2019**, *2019*, 2071–2080.
[58] B. Liegault, D. Lapointe, L. Caron, A. Vlassova, K. Fagnou, *J. Org. Chem.* **2009**, *74*, 1826–1834.
[59] M. Lafrance, D. Lapointe, K. Fagnou, *Tetrahedron* **2008**, *64*, 6015–6020.
[60] R. Thakuria, N. K. Nath, B. K. Saha, *Cryst. Growth Des.* **2019**, *19*, 523–528.
[61] C. D. Sherrill, *Acc. Chem. Res.* **2013**, *46*, 1020–1028.
[62] C. Erker, T. Basché, *J. Am. Chem. Soc.* **2022**, *144*, 14053–14056.
[63] D. G. Congrave, B. H. Drummond, V. Gray, A. D. Bond, A. Rao, R. H. Friend, H. Bronstein, *Polym. Chem.* **2021**, *12*, 1830–1836.
[64] Y. He, W. Xu, I. Murtaza, C. Yao, Y. Zhu, A. Li, C. He, H. Meng, *J. Mater. Chem. C* **2018**, *6*, 3683–3689.
[65] M. Kato, N. Fukui, H. Shinokubo, *Chem. Eur. J.* **2022**, *28*, e202103647.
[66] F. Alvarez-Ramírez, Y. Ruiz-Morales, *J. Chem. Inf. Model.* **2019**, *60*, 611–620.

Manuscript received: October 29, 2024
Revised manuscript received: December 26, 2024
Accepted manuscript online: January 8, 2025
Version of record online: January 20, 2025